PAPER

Fructose recognition using new "Off–On" fluorescent chemical probes based on boronate-tagged 1,8-naphthalimide

Sanaz Seraj,[a] Shohre Rouhani (ID) *[ab] and Farnoush Faridbod (ID) [c]

It has recently been found that hereditary fructose intolerance (HFI) alongside the blood glucose level can be an important indicator in diabetes or some metabolic disorders. Over time, fluorescent organic molecules have grown in popularity for selective recognitions of a wide range of analytes. This work introduces new synthesized molecules based on boronate-tagged 1,8-naphthalimide with a planar structure and high fusion loops for rapid optical detection of fructose. Boronic acids which form five-membered boronate esters with diols have become increasingly popular in the synthesis of small chemical receptors. Two new water-soluble fluorescent selectophores have been successfully synthesized and their selectivity has been studied in sensing saccharides. The synthesized selectophores indicated selectivity toward fructose compared to other tested saccharides within the range of 0.16 to 50 mM at the physiological pH 7.4. The designed fluorescent probes were used to measure the percentage of fructose in fructose corn syrup. The results revealed that the (2-(((2-((7-oxo-7*H*-benzo[*d,e*]benzo[4,5]imidazo[2,1-*a*]isoquinolin-3-yl)amino)ethyl)amino)methyl)phenyl)boronic acid (NONB) probe was able to determine the concentration of fructose satisfactorily, suggesting that this probe can potentially be applied for quantitative detection of fructose in real samples.

Introduction

Carbohydrates are one of the three main categories of biomolecules that are essential in biological systems. Glucose and fructose levels play a significant role in some diseases, such as hypoglycemia, diabetes mellitus, and hereditary fructose intolerance (HFI). Therefore, quantitative monitoring of saccharides such as fructose is of great importance in diagnoses and therapies.[1,2] HFI is due to a deficiency of fructose-1-phosphate aldose activity which can cause accumulation of fructose in the liver, small intestine, and kidneys. This disease is currently diagnosed with an H2-exhalation test. This test is dangerous to the patient and causes complications such as the use of fructose by the patient during the test. On the other hand, only limited laboratories have the ability to detect the disease at the blood level by molecular biological diagnostic methods. For that reason, monitoring blood fructose levels is of great relevance.[3,4] Development of small molecules which are able to

interact selectively with carbohydrates requires special recognition moieties capable of strong binding under physiological conditions. Many molecules and biomolecules have been reported for saccharide detection including antibodies,[5] lectins,[6] aptamers based on nucleic acids[7] and small molecule lectin mimics,[8] and boronic acids and derivatives.[9–11] Among the above-mentioned materials, boronic acid compounds have attracted more interest thanks to their strong interactions with sugars. Boronic acids can bind tightly and reversibly to *cis*-1,2 or 1,3 diol moieties to form five- or six-membered rings, respectively.[12–14] The fluorescence of boronic acid-based compounds changes when bound with sugars.[15–21] According to these properties, they have been used for a wide variety of applications including solution carbohydrate sensing,[22,23] cell labeling based on cell surface carbohydrate biomarkers,[24] and carbohydrate separation.[25] The first fluorescence sensor for saccharide detection was designed by Czarnik in 1992.[26] In this design, the boronic acid group was directly attached to the anthracene ring. After that, various fluorescence probes were made by Shinkai and coworkers.[27,28] The designed probes had high fluorescence emission, which was quenched in the presence of fructose. After the investigation by Shinkai, different fluorescence probes were developed to detect saccharides.[29,30] One of the major challenges in designing probe studies was the lack of fluorescence emission changes. To improve this problem, the photoinduced electron transfer (PET)

[a] *Department of Organic Colorants, Institute for Color Science and Technology, Tehran, Iran. E-mail: rouhani@icrc.ac.ir*

[b] *Center of excellence for Color Science and Technology (CECST), Institute for Color Science and Technology, Tehran, Iran*

[c] *Center of Excellence in Electrochemistry, School of Chemistry, College of Science, University of Tehran, Tehran, Iran*

mechanism was introduced by James and coworkers in 1994.[31] Based on this mechanism, the probe is designed in three parts including donor, spacer, and acceptor. They used the amine group as a Lewis base and boronic acids as a Lewis acid for the first time.[32] 1,8-Naphthalimide is well known for its typical photoinduced electron transfer (PET) and intramolecular charge transfer (ICT), strong absorption and emission in the visible region and large Stokes shift. Design, synthesis, and application of some 1,8-naphthalimide derivatives for sensor applications have been undertaken by our team.[33–35] Until now, various fluorescent probes including a boronic acid group based on naphthalimide dyes have been designed and developed to detect monosaccharides.[15,17,36–39] In recent years, the use of different structures to improve the PET mechanism, the type of interactions between the amine and boron groups and the effect of an amine group on the detection rate of saccharides has become a very attractive field. On the other hand, the design of fluorescent chemical sensors for neutral organic species presents a more serious challenge due to the lack of sufficient electronic changes upon inclusion. Saccharides are generally soluble in polar protic solvents but such solvents are competitive with the guest in a hydrogen bonding receptor. However, the design of a fluorescence chemical sensor based on the boronic acid–saccharide interaction has been difficult due to the lack of sufficient electronic variations found in either the boronic acid moiety or the saccharide moiety. These above-mentioned disadvantages of boronic acid–saccharide interactions can be overcome by modifying the boronic acid binding site to create an electron-rich center around the boronic acid moiety. Given the stronger acidity of boronic acid upon polyol-binding as well as the tight and reversible binding between sugars and boronic acid, we synthesized two PET probes for the measuring of saccharides. A new water-soluble naphthalimide dye was designed with fused loops. Increasing the number of rings in the naphthalimide fluorophore can lead to greater electron absorption from the electron-rich center at the lower part of the molecule to create a probe with low fluorescence intensity based on the PET mechanism. In addition, a nitrogen around the boronic acid moiety in the (2-(((2-((7-oxo-7H-benzo[d,e]benzo[4,5]imidazo[2,1-a]isoquinolin-3yl)amino)ethyl)amino)methyl)phenyl)boronic acid (NONB) probe and sulphur around the boronic acid moiety in the 4-thiophene-N-propyl (triethoxysilane)1,8-naphthalimide (NST) probe were designed. The effects of the designed groups for detection of monosaccharides are discussed further.

Experimental

Materials

Acenaphthene, ortho-phenylenediamine, and bromomethyl-phenyl boronic acid pinacol ester were purchased from Merck Chemical Co. and used as received. All solvents were of analytical grade. 2-5-Thiophenediyl-bisboronic acid was purchased from Aldrich Co. The following experiments were conducted in PBS/DMF (99 : 1).

Equipment

All fluorescence spectral measurements were performed using a Perkin-Elmer LS55 fluorescence spectrophotometer. UV-Vis absorption of the synthesized dyes in PBS solution was collected on a CECIL-CE9200 spectrophotometer. ^{1}H NMR and ^{13}C NMR spectra were recorded using a Brucker DRX AVANCE NMR spectrophotometer at 500 MHz and 125 MHz in DMSO. FTIR spectra were recorded on a SPECTRUM ONE spectrometer using KBr pellets. Fluorescence quantum yield was evaluated based on the absorption and fluorescence spectra, using fluorescein as a reference (φ_{st} = 0.95).[40] The melting points (m.p.) were determined using a Perkin-Elmer (USA) Pyris 6 differential scanning calorimeter.
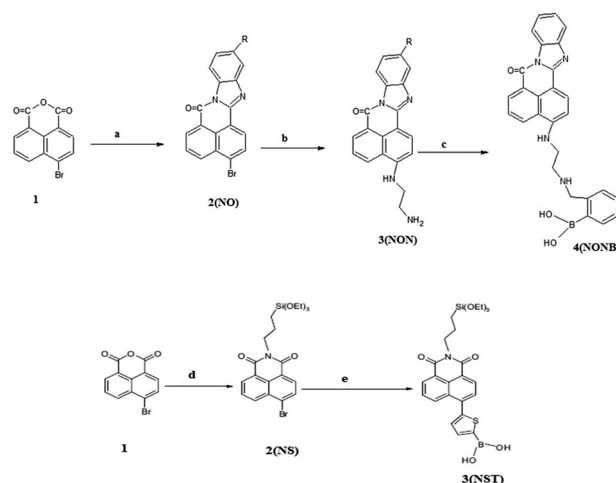
Synthesis

The intermediate compound **1** (as shown in Scheme 1) was synthesized from acenaphthene according to the literature.[41–43] The synthesis of the fluorescent probes is also illustrated in Scheme 1.

Synthesis of 3-(and 4-) bromo-7H-benzimidazo[2,1-a] benz[d,e]-isoquinolin-7-ones (NO). 4-Bromo-1,8-naphthalic anhydride (36 mmol) and o-phenylene diamine (55 mmol) were refluxed in glacial acetic acid (120 ml) for 7 h and washed off with water to obtain the desired product. The crude product was recrystallized with acetic acid to yield the compound NO (73%).

Synthesis of 3-(and 4-)(2-aminoathylamine)-7H-benzimid-azo(2,1-a)benz(d,e) iso-quinolin-7-ones (NON). NO (0.17 mmol), ethylenediamine (5 ml) and CuSO₄·5H₂O (0.2 g) were refluxed in 2-methoxyethanol (100 ml) for 10 h. The liquor was poured into water to yield NON dye recrystallized from toluene as orange needles (57%).

Synthesis of (2-(((2-((7-oxo-7H-benzo[d,e]benzo[4,5]imidazo[2,1-a]isoquinolin-3yl)amino)ethyl)amino)methyl)phenyl) boronic acid (NONB). The NONB probe was synthesized by refluxing

Scheme 1 Synthesis procedure for the NONB and NST probe: (a) o-phenylenediamine, glacial acetic acid, reflux 7 h, 73%; (b) ethylene diamine, 2-methoxyethanol, reflux 10 h, 57%; (c) (2-bromomethylphenyl) boronic acid pinacol ester, dry THF/MeOH, reflux 6 h, 25%; (d) APTS, ethanol, 85% (e) thiophene-2,5-diyldiboronicacid, Pd(PPh₃), toluene, reflux, 28 h.

compound NON (0.56 mmol) with (2-bromomethylphenyl) boronic acid pinacol ester (0.94 mmol) in a 40 ml mixed solution of THF:CH_3OH (v:v = 1:1). Then, 2 ml of triethylamine was added drop-wise to the above solution for 6 h. The solvent was removed under reduced pressure and the product was purified on silica gel using [5:1 CH_2Cl_2:CH_3OH] to yield orange powders (25%).

Synthesis of 4-bromo-*N*-propyl (triethoxysilane)1,8-naphthalimide (NS). The intermediate compound NS was prepared by the reaction of 0.275 mmol of compound **1** with 2.2 mmol of 3-aminopropyl-triethoxysilane in ethanol. The solvent was evaporated *via* rotary evaporation and the crude product was recrystallized with ethanol to generate compound NS (85%).[44]

Synthesis of 4-thiophene-*N*-propyl (triethoxysilane)1,8-naphthalimide (NST). The NST compound was synthesized *via* the palladium-catalyst Suzuki reaction.[45] The intermediate (NS) (0.5 mmol), Pd(PPh$_3$)$_4$ (0.01 mmol), K$_3$PO$_4$ (0.75 mmol) and 2,5-thiophenediyl-bisboronic acid (0.75 mmol) in DMF were mixed, stirred, and refluxed for 28 h. The crude products were then concentrated under vacuum and further purified by chromatography on silica gel with a solution of CH_2Cl_2 and CH_3OH as a diluent.

Results and discussion

General procedure for synthesis of the fluorescent probes

The general procedure for the synthesis of NONB and NST is displayed in Scheme 1. 4-Bromo-1,8-naphthalic anhydride (1) was prepared according to the procedure reported previously.[44–47] Compound NO was obtained by the reaction of compound **1** with *ortho*-phenylenediamine in glacial acetic acid. Compound NONB was synthesized by the condensation of compound NO with (2-bromomethylphenyl) boronic acid pinacol ester in THF:CH_3OH (v:v = 1:1). Next, compound NS was synthesized *via* the reaction of compound **1** with APTS in ethanol. Finally, compound NST was prepared *via* the condensation of compound NS with thiophene-2,5-diyilboronic acid, catalyzed by Pd(PPh$_3$)$_4$ in DMF.

Synthesis of 3-(and 4-) bromo-7*H*-benzimidazo[2,1-*a*] benz[*d,e*] isoquinolin-7-ones (NO). Yield (73%), yellow needles, m.p. 215–216 °C, FTIR (KBr) cm^{-1}: 3055 (Ar C–H st), 1712 (C=O), 1695 (C=N), 1227 (C–N), 706 (C–Br). ^{1}H NMR (DMSO, 500 MHz) δ ppm: 8.79–8.74 (1H, m, naphthyl ring), 8.61–8.63 (1H, m, naphthyl ring), 8.47–8.50 (1H, m, naphthyl ring), 8.39 (1H, m, naphthyl ring), 8.21–8.28 (1H, m, naphthyl ring), 8.99–8.05 (1H, m, Ar-H), 7.86 (1H, m, Ar-H), 7.50 (2H, m, Ar-H). Elemental analysis: Anal. calcd (%) for: C$_{18}$H$_9$BrN$_2$O: C, 61.91; H, 2.59; N, 8.02. Found: C, 61.88; H, 2.55; N, 8.11.

Synthesis of 3-(and 4-)(2-aminoathylamine)-7*H*-benzimidazo(2,1-*a*) benz (*d,e*) iso-quinolin-7-ones (NON). Yield (57%), orange needles, m.p. 207–208 °C, FTIR (KBr) cm^{-1}: 3500 (–NH$_2$–), 2940 (CH$_2$), 1700 (C=O). ^{1}H NMR (DMSO, 500 MHz) δ ppm: 9.41 (2H, s, naphthalimide–NH–) 8.27–7.31 (5H, m, naphthyl ring), 7.55–7.21 (4H, m, imidazole ring), 3.31 (2H, t, ethylene), 2.73 (2H, t, ethylene), 1.49 (2H, s, amine –NH$_2$). Elemental analysis:

Anal. calcd (%) for: C$_{20}$H$_{16}$N$_4$O: C, 73.17; H, 4.88; N, 17.07. Found (%): C, 73.15; H, 5.11; N, 16.98.

Synthesis of (2-(((2-((7-oxo-7*H*-benzo[*d,e*]benzo[4,5]imidazo [2,1-*a*]isoquinolin-3-yl)amino)ethyl)amino)methyl)phenyl) boronic acid (NONB). Yield (25%), orange powders, m.p. 140–141 °C, λ_{max} (logε) = 467 nm, FTIR (KBr) cm^{-1}: 3200–3400 (–NH st and BO-H st), 3056 (aromatic C–H st), 2919 (aliphatic C–H st.), 1712 (C=O), 1695 (C=N), 1227 (C–N), 3430 (OH), 1100 (B–O), 659 (B–C). ^{1}H NMR (DMSO, 500 MHz) δ ppm: 9.46 (1H,s, naphthalimide–NH–), 7.21–8.27 (13H, m, Ar-H), 4.21 (2H, s, –OH), 4.16 (1H, s, –NH–), 3.77 (2H, s, –CH$_2$–), 3.36 (2H, t, –CH$_2$–), 2.64 (2H, t, –CH$_2$–). Elemental analysis: Anal. calcd (%) for: C$_{27}$H$_{24}$N$_4$O: C, 80.20; H, 5.94; N, 13.86. Found (%): C, 80.24; H, 5.92; N, 13.90.

Photophysical properties

NONB and NST dyes, as probes, are designed based on the photoinduced electron transfer (PET) mechanism inhibition. Sensors based on the PET mechanism are in the fluorophore–spacer–receptor format.[48–50] If PET occurs between the fluorophore and the receptor, the fluorescence emission of the dye turns off. If it can occur efficiently, the fluorescence of the fluorophore will be quenched. When the receptor binds to the guest molecule, the PET in the system is inhibited and the fluorescence intensity grows. Nowadays, PET is one of the most extensively adopted mechanisms for the development of chemical bulk sensors. When an electron donating group is substituted on the naphthalimide ring, it usually enhances the PET mechanism at the C-4 position. Amine and thiophene groups in the 4-position can enhance the fluorescence properties and acts as a donor group while the carbonyl group can act as the acceptor group. *N*-Substituted 1,8-naphthalimide is an excellent D–π–A chromophore with good photophysical and photochemical properties. 1,8-Naphthalimide is a polar molecule in both the ground and excited states. Substitution of electron donating or electron withdrawing groups at the C-4 position of the naphthalimide core strongly affects their emission spectra. Fig. 1 demonstrates the absorption and emission spectra of NONB and NST probes. The Stokes shifts for the NONB probe and NST probe are large enough to avoid self-quenching. On the other hand, the fluorescence quantum yields of NONB and NST (Table 1) in PBS were relatively low, suggesting the potential of both probes in the detection of saccharides under physiological conditions.

The water solubility of both designed probes in PBS 50 mM (pH = 7.4) was examined by measuring the absorbance of the probes at various concentrations (0–3 × 10^{-2} mM) according to the Beer Lambert law. Fig. 1 indicates that both probes were completely soluble in PBS within the concentration range of (0–3 × 10^{-2} mM) (5 × 10^{-2} mM was used in this work). Therefore, the subsequent tests were conducted at pH = 7.4 PBS/DMF (99:1). The structure of the NONB and NST probes, called selectophores, are displayed in Scheme 2.

Sensing properties

Spectral response of the fluorescent probes toward sugars. In order to study the sensing properties of the synthesized
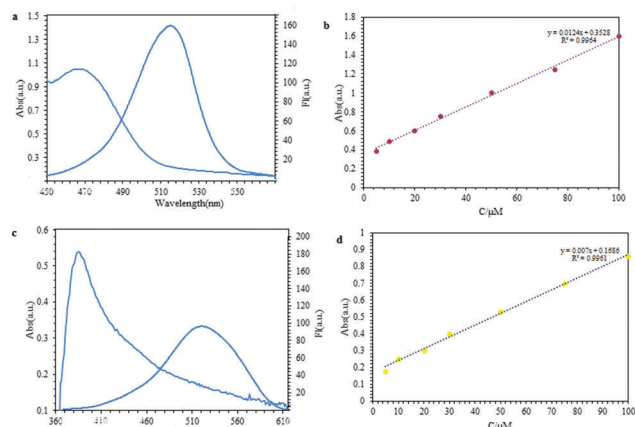
Fig. 1 (a) Absorption and emission spectra of the NONB probe in PBS, [NONB] = 5 × 10⁻² mM, λ_{exNONB} = 391 nm, 50 mM PBS, pH = 7.4, (b) the linear correlation between the absorbance and the NONB probe concentration, 50 mM PBS, pH = 7.4, (c) absorption and emission spectra of the NST probe in PBS, [NST] = 5 × 10⁻² mM, $\lambda_{ex\,NST}$ = 379 nm, 50 mM PBS, pH = 7.4, and (d) the linear correlation between the absorbance and the NST probe concentration, 50 mM PBS, pH = 7.4.

Table 1 The association constants (K_{as}) between NONB and NST with fructose and their detection limits (LOD) and quantum yield in the presence and absence of fructose

Probe	K_{as} (M⁻¹)	LOD (mM)	φ_{fa}[a]	FE[b]
NONB-fructose	80.64	0.049	0.2	2.22
NONB blank	—	—	0.09	—
NST-fructose	35.84	0.1	0.14	2
NST blank	—	—	0.07	—

[a] Fluorescein (φ = 0.95 in ethanol) was used as the reference, [NONB] = 5 × 10⁻² mM, [NST] = 5 × 10⁻² mM, [fructose] = 100 mM, 50 mM PBS, pH 7.4. [b] Fluorescent enhancement (FE) is the ratio of quantum yield with sugar and that without sugar.

fluorophores (NONB and NST), and introduce them as selectophores, the probes (10⁻² mM in PBS solution) were titrated by different concentrations of D-fructose. As shown in Fig. 2, by increasing the fructose concentration, the absorption of both probes grew.
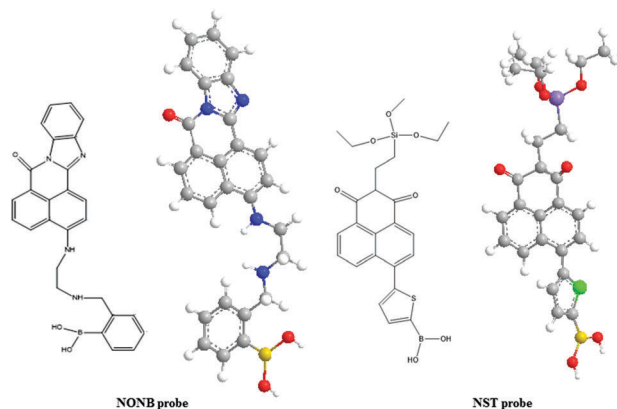
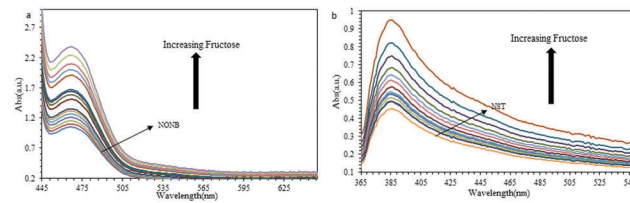**Scheme 2** Structure of the NONB and NST selectophores.

Fig. 2 (a) UV-Vis spectral changes of NONB in the presence of different concentrations of D-fructose (0–2 M), [NONB] = 5 × 10⁻² mM, 50 mM PBS, pH 7.4, λ_{ex} = 391 nm, and (b) UV-Vis spectral changes of NST in the presence of different concentrations of D-fructose (0–2 M), [NST] = 5 × 10⁻² mM, 50 mM PBS, pH 7.4, λ_{ex} = 379 nm.
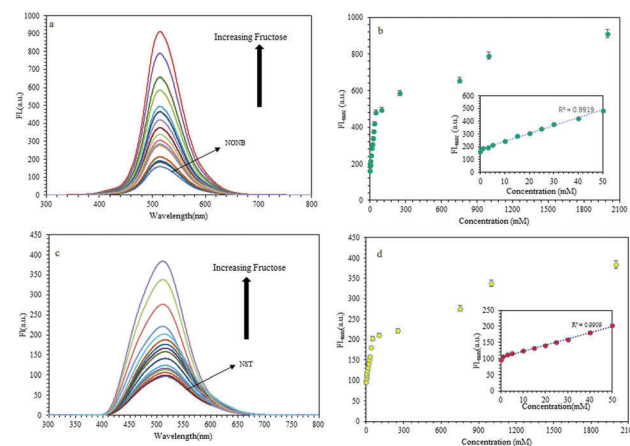

Fig. 3 (a) Fluorescence change of NONB (5 × 10⁻² mM) in the presence of D-fructose (0–2 M) in PBS (50 mM, pH 7.4), (b) linear range of the fluorescence change of NONB at 514 nm in the presence of D-fructose (λ_{ex} = 391 nm), (c) fluorescence change of NST (5 × 10⁻² mM) in the presence of D-fructose (0–2 M) in PBS (50 mM, pH 7.4), and (d) linear range of the fluorescence change of NST at 515 nm in the presence of D-fructose (λ_{ex} = 379 nm).

The fluorescence emission of the probes revealed enhancements upon the addition of 0–2 M of D-fructose. The fluorescence titration spectra of NONB and NST with various amounts of D-fructose are displayed in Fig. 3. Fluorescence enhancements of both probes are observed upon the addition of D-fructose. The introduction of D-fructose induced about 6.4-fold and 4-fold fluorescence enhancements for NONB and NST, respectively. The relative signal changes in transitioning from zero to 100 mM of D-fructose are highly dependent on buffer pH (Fig. 4). By varying the pH from 2 to 11, the fluorescence of the probes without D-fructose is higher at acidic pH than at neutral and basic pHs. In probes based on the PET
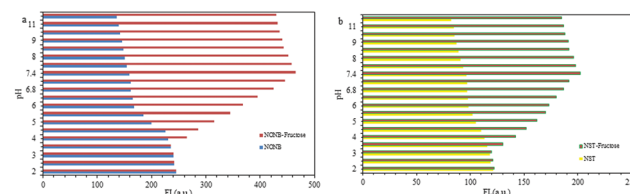

Fig. 4 Fluorescence change of NONB and NST probes in the presence of D-fructose in 50 mM PBS with different pH values.

mechanism, with reduction of pH, the donor moiety at the end of the molecule would be protonated; PET is interrupted and the fluorescence emission grows. As a result, enhanced fluorescence emission confirms the performance of the probes according to the PET mechanism by decreasing the pH. In the absence of any sugar, the fluorescence intensity of NONB and NST diminished upon altering the pH from 2 to 11. Also, an apparent pK_a of 7.8 was observed for NST, which is assigned to the boronic acid moiety. An apparent pK_a of 6 was observed for NONB. In the presence of fructose, the fluorescence intensity was tested within the pH 2–11 region. The fluorescence intensity increased with elevation of pH. An apparent pK_a of 5.5 for NST and 4 for NONB were observed. As has been demonstrated by past studies, boronic acids with lower pK_a values tend to have higher binding constants. The apparent pK_a of 6 for NONB was lower than that of NST (7.8) determined under similar conditions. Due to the presence of a nitrogen group near the boron atom, the NONB probe has been able to reduce pK_a to 4 when binding to fructose. The nitrogen atom has formed a dative bond with the boron atom, resulting in a reduction in the pK_a. However, the NST probe only dropped to 5.5, due to the lack of binding between the sulfur atom and the boron atom when linked to the fructose. As a result, the greater reduction in the pK_a of the NONB probe because of the N···B bonding can probably lead to a higher binding constant as compared to the NST probe. According to the results, the neutral pH (7.4) was selected for the following experiments.

Selectivity

To investigate the selectivity of both probes, the fluorescence emission changes were evaluated in the presence of different sugars. As illustrated in Fig. 5, in the presence of 50 mM of fructose, sorbitol, mannose, glucose, galactose, and glucosamine, the designed probes only showed fluorescent changes toward fructose. However, as can be observed, no significant changes occurred in the case of other saccharides.

The behavior of NONB and NST probes against saccharides follows a trend that is typical for aromatic boronic acids, where its affinity is as follows: D-fructose > sorbitol > D-galactose > D-glucose > mannose > glucoseamine. The selectivity patterns represent the reorganization of the diol (cis or trans configuration), and the sterical hindrance via e.g. the hydroxymethyl group of the saccharides.[51]

The binding interaction between the probes and fructose was further studied via association constant measurement (Fig. 6).
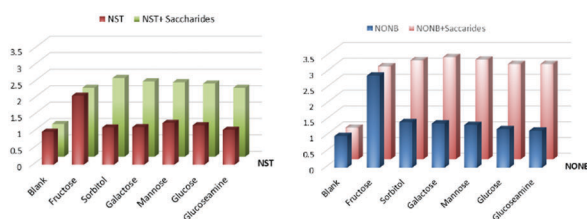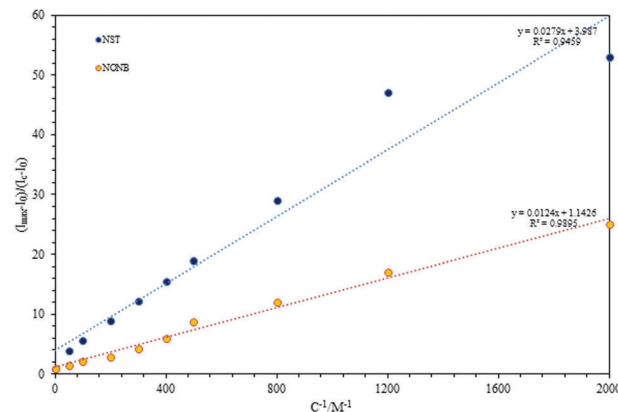

Fig. 6 Plots of $(I_{max} - I_0)/(I_c - I_0)$ against c^{-1} for NONB and NST probes with fructose sugar. [NONB] = [NST] = 5×10^{-2} mM, [fructose] = 50 mM, 50 mM PBS, pH 7.4.

As displayed in Fig. 6, the line slope for the NONB probe is less than that of the NST probe. On the other hand, the association constant value of the NONB probe is greater than that of the NST probe. According to the results obtained, the line slope and the association constant values, the sensitivity of the NONB probe to fructose is greater than that of the NST probe.

The linear response ranges for the NONB probe were obtained within [0.16–50 mM] with a regression $R^2 = 0.991$, and the linear response ranges for the NST probe were found within [0.34–50 mM] with a regression $R^2 = 0.988$. The association constant, the detection limit (LOD) and quantum yield (Q_y) in the presence of fructose were measured and outlined in Table 1.

LOD was measured using the equation $3S_b/K$ where S_b is the standard deviation of the blank. A total of 10 measurements were carried out, where K is the slope of the fitted area. Fluorescence measurements as well as the association constant and LOD suggest that the NONB probe has a lower detection limit than NST for fructose detection. The results of Fig. 5 indicate a selectivity to fructose for both probes. Furthermore, 10 replicate measurements of 100 mM fructose yielded a reproductive intensity with the relative standard deviation (R.S.D) of 1.31% and 1.2% for NONB and NST, respectively. Furthermore, five independent optical sensors were prepared using the same procedure and used for the determination of fructose (100 mM) with the R.S.D of 1.7 and 1.8% for NONB and NST, respectively, suggesting good repeatability and reproducibility of this current optical sensor.

Sensing mechanism

Boronic acids are capable of binding to compounds containing diol groups through the formation of reversible ester compounds.

The interaction between boronic acid and diol is highly pH-dependent. The boronic acid group is an electron-deficient Lewis acid with a sp^2-hybridized boron atom and a trigonal structure. With the increase of pH, the anionic form of boronic acid develops with a more electron rich sp^3-hybridized boron atom with a tetrahedral structure. The changes in the electronic and structural properties in the boron atom influence the

Fig. 5 Intensity changes of NONB (5×10^{-2} mM) and NST (5×10^{-2} mM) upon addition of different saccharides (50 mM) in PBS (50 mM, pH7.4) in the absence and presence of (50 mM) fructose.
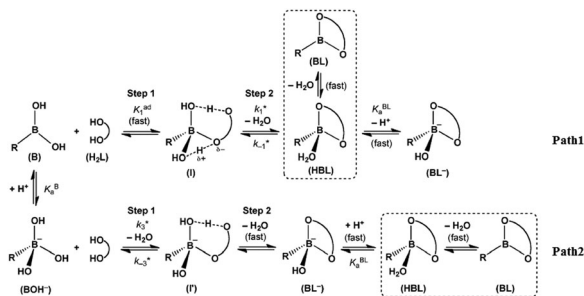
Scheme 3 Reaction mechanism of boronic acid with diol with high pK_a in alkaline solution.[45]

fluorescence emission changes in the probes.[52] The interaction mechanism of the boronic acid with diol is illustrated in Scheme 3. As revealed in Scheme 3, in the reaction systems consisting of phenylboronic acid (pK_a = 8.72) with fructose (pK_a = 12.3) at pH = 7.4, the problem of proton ambiguity is resolved, as the ligand concentrations are [$H_2L \gg HL^-$] at pH = 7.4 and the kinetics reactivity order is $H_2L > HL^-$. With reference to Scheme 3, the structure changes from the state of trigonal ($RB(OH)_2$) to the tetrahedral state (intermediate I). With the structure change, the coordination number varies from three to four, where these changes occur very fast. It is followed by rate-determining chelate-ring closure in the tetrahedral intermediate I to form intermediate HBL, which may be in fast trigonal-tetrahedral equilibrium with the chelated trigonal species (BL).[53] The stability of the boronate ester is pH dependent. The optimal pH for the binding of boronic acid compounds to diols is above the pK_a of the boronic acid species. Therefore, reduction of the pK_a of a boronic acid is known to increase the binding constant of boronic acids.[45] Conversion of the boronic acid to the ester results in diminished pK_a.[53] When using boronic acid with a high pK_a value (pK_a = 7–9), $RB(OH)_2$ is always reactive irrespective of the pH of the solution; it is reactive in a strong alkaline solution since the reactivity of $RB(OH)_2$ is far higher than that of $RB(OH)_3^-$. In this study, we used the neutral pH and boronic acid with a high pK_a value (pK_a = 7–9) and we expect the $RB(OH)_2$ (trigonal form) formation to be greater than the $RB(OH)_3^-$ formation (tetrahedral form). As has been concluded by past studies, boronic acids with lower pK_a values tend to have higher binding constants. The apparent pK_a of NONB (6) is lower than that of NST (7.8) in the absence of sugars determined under similar conditions. This might be a major contributing factor to the higher binding constant for NONB toward fructose. A further decrease of pK_a yields further increase in the sugar binding constant. For this reason, the NONB probe including a nitrogen moiety reduces the pK_a to 4 and the NST probe including a sulfur moiety decrease the pK_a to 5.5. As a result, the NONB probe has a higher sugar binding constant than the NST probe. The reason is that the sulfur atom can be weakly bonded to the boron atom.[54] However, with the reaction between boronic acid and fructose, the Lewis acidity of boron increases and the nitrogen heteroatom can create a dative bond with the free orbit of boronic acid, where this bond formation leads to a further reduction in pK_a

(in the presence of fructose). For this reason, the NONB probe with the nitrogen moiety near to the boron atom has a higher sugar binding constant than that of the NST probe with a sulfur moiety. Consequently, the NONB probe tends more positively to the trigonal form due to the dative bond formation (by lowering the pK_a) and a more stable complex is established in the presence of a nitrogen atom with the sugar molecule. In addition to the presence of the nitrogen group in reducing pK_a, in the structure of the NONB probe, with the closure of the naphthalimide rings and the increase in rings, the probe becomes more rigid. However, there is a flexible chain on the top of the naphthalimide loop in the NST probe. Increasing the rigidity of the NONB structure helps to strengthen the PET mechanism and the electrons are stretched with more power from the receptor. The NONB probe examined in this study had a lower detection limit in detecting saccharides compared to other fluorescent probes in other studies. Thus, this probe can potentially be a good candidate for measuring fructose in real samples at physiological pH. The binding of the designed probes with fructose is shown in Scheme 4.
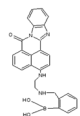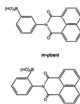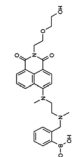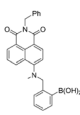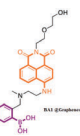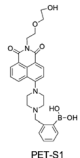
The studies performed on naphthalimide fluorescence probes containing boronic acids for the detection of fructose are shown in Table 2.

As reported in Table 2, the performance of the fluorescence probe designed in the present work was in most cases better than the previous literature. A study conducted in 2002 focused on the position of the group of boronic acids placed above the naphthalimide ring in the *ortho* and *para* positions. Since 2006, various naphthalimide dyes have been designed based on the PET mechanism for the detection of fructose. In this research work, more fused loops were used for the first time in the detection of saccharides in comparison with other studies on improving the performance of naphthalimide dyes based on the PET mechanism. The presence of fused loops causes stronger PET in the system due to higher rigidity of the
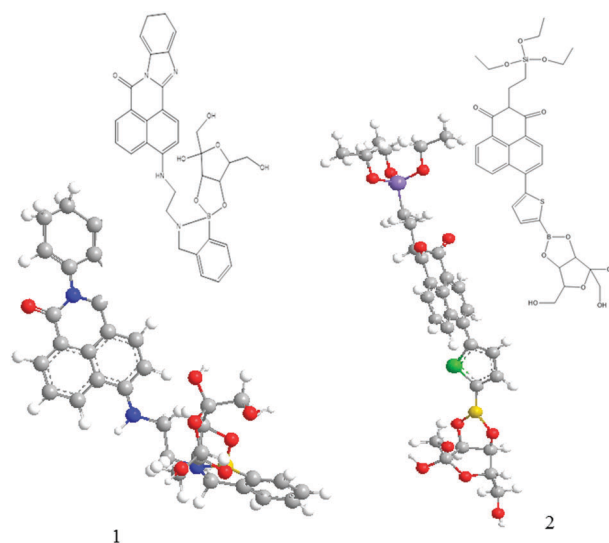
Scheme 4 Binding of fluorescent probes with fructose: (1) NONB and (2) NST.

Table 2 Naphthalimide fluorescent probes for fructose detection

Structure	Stock shift (nm)	Mechanism of detection	pH	Association constant (K_a (M^{-1}))	Linear range (mM)	ΔI_f	LOD (mM)	Year	Ref.
	50	Flourescence enhancement	7.4	80.64	0.16–50	3.5	0.049	2018	This work
	55	Quenching	7.5	1.6, 1.3	NR	—	—	2002	32
	120	Flourescence enhancement	7.5	170	1–20	2	0.1 mM	2006	15
	77	Flourescence enhancement	7.4	57	NR	2.5	2–2.3 M	2007	30
	77	Flourescence enhancement	7.4	28	NR	2.5	—	2008	31
	85	Flourescence enhancement	9	NR	0–50 mM	2.8	2.7	2014	29
	130	Flourescence enhancement	7.4	75.8	0–2000	50	0.045	2015	17

NR = no report.

backbone of the dye and greater reduction in the initial fluorescence of the dye, resulting in a further increase in fluorescence emission and a lower detection limit by binding to the sugar molecule. In addition to their remarkable fluorescence properties, they are known as an important class of drugs in antitumor therapy and thus characterized by high cytotoxicity activity against a variety of tumor cells[55] due to the presence of a coplanar fluorophore, π-deficient aromatic system and one or two basic side chains, some of which have shown promising antitumor activities. On the other hand, a new generation of probes for saccharide detection with drug activity and a lower detection limit has the potential to be created and studied. This new structure can also be used in the fluorescence imaging of carbohydrates in future studies.

The LOD of this sensor is 0.049 mM (0.45 ppb) for fructose. Chromatography is the general method for all sugar analysis.

Different chromatographic methods were developed for saccharide determination. Some of the analytical methods for fructose determination are described in Table 3, and as can be seen the present work can detect low amounts of fructose and is a suitable candidate for developing a new sensing method for fructose detection.

Table 3 Comparing the LODs of different analytical techniques for fructose

Techniques	LOD	Ref.
HPLC-RI	57.86 mg L^{-1}	56
LC	3.0 mg L^{-1}	57
HPLC-RID	0.03–0.56 mg L^{-1}	58
HPLC -SPE	$(3.30–16.48) \times 10^3$ mg L^{-1}	59
Fluorescence sensor	0.049 mM (0.00045 mg L^{-1})	This work

Analytical performance of the optical probes

To check the analytical performance of the probes in real matrixes, the fructose content of a standard solution of fructose, named high-fructose corn syrup 55 (HFCS-55) was determined using the standard addition method. As expected, the NONB probe was able to determine the fructose concentration of the standard fructose sample successfully (the relative error was less than 4.7% for three replicate measurements). This suggests that this probe can potentially be used for quantitatively detecting fructose levels in real samples like blood and urea.

Conclusions

In summary, we developed selective "turn-on" fluorescence sensors for fructose detection by novel naphthalimide probes based on photoinduced electron transfer. The photophysical characteristics of the dyes were evaluated in the presence of fructose. The probe including the amine moiety near the boron atom revealed greater selectivity and sensitivity to fructose than the probe including a sulfur moiety. The remarkable enhancement in the fluorescence intensity of the NONB probe upon the addition of fructose makes it potentially a good candidate for fabricating a highly sensitive and selective probe for quantitatively detecting fructose levels in real samples such as blood and urea.

Conflicts of interest

There are no conflicts to declare.

Acknowledgements

Notes and references

1 C. Tran, *Nutrients*, 2017, **9**, 356–366.
2 T. Mogos and A. Evelin Iacobini, *Rom J. Diabetes Nutr. Metab. Dis.*, 2016, **23**, 081–085.
3 H. Li, H. M. Byers and A. Diaz, *Mol. Genet. Metab.*, 2018, **123**, 428–432.
4 A. Quaglia, E. A. Roberts and M. Torbenson, *Macsween's Pathology of the Liver, Developmental and Inherited Liver Disease*, 7th edn, 2018, ch. 3, pp. 111–274.
5 U. Boas, P. Lind and U. Riber, *Anal. Biochem.*, 2014, **465**, 73–80.
6 Q. Hou, J. Wang, X. Liu and Z. Wang, *Chem. Res. Chin. Univ.*, 2012, **28**, 947–952.
7 W. Sun, L. Du and M. Li, *Curr. Pharm. Des.*, 2010, **16**, 2269–2278.
8 C. Ke, H. Destecroix, M. Crump and A. Davis, *Nat. Chem.*, 2012, **4**, 718–723.
9 Z. Xu and P. Deng, *Mater. Sci. Eng.*, 2014, **40**, 228–235.
10 C. H. Wang and H. Zhu, *Anal.*, 2013, **138**, 7146–7151.
11 H. Chen and L. Li, *RSC Adv.*, 2015, **5**, 13085–13092.
12 W. Zhai, X. Sun, T. D. James and J. S. Fossey, *Chem. – Asian J.*, 2015, **10**, 1836–1848.
13 J. P. Lorand and J. Q. Edwards, *J. Org. Chem.*, 1959, **24**, 769–774.
14 S. D. Bull, M. G. Davidson, J. M. H. Van Denelson, J. S. Fossey, A. T. A. Jenkins, Y. Jiang, Y. Kubo, F. Marken, K. Sakurai, J. Zhao and T. D. James, *Acc. Chem. Res.*, 2013, **46**, 312–326.
15 S. Trupp, A. Schweitzer and J. Mohr, *Org. Biomol. Chem.*, 2006, **4**, 2965–2968.
16 X. Gao, Y. Zhang and B. Wang, *New J. Chem.*, 2005, **29**, 579–586.
17 H. Chen, L. Li, H. Guo, X. Wang and W. Qin, *RSC Adv.*, 2015, **5**, 13805–13811.
18 Y. J. Huang, W. J. Quyang, X. Wu, Z. Li, J. S. Fossey, T. D. James and Y. B. Jiang, *J. Am. Chem. Soc.*, 2013, **135**, 1700–1721.
19 L. N. Neupane, S. Y. Han and K. H. Lee, *Chem. Commun.*, 2014, **50**, 5854–5862.
20 J. S. Hansen, M. Ficker, J. F. Peterson, J. B. Christensen and T. Hoeg-Jensen, *Tetrahedron Lett.*, 2013, **54**, 1849–1862.
21 B. Xu, J. Hou, K. Li, Z. Lu and X. Yu, *Chin. J. Chem.*, 2015, **33**, 101–111.
22 G. Kaur, H. Fang, X. Gao, H. Li and B. Wang, *Tetrahedron*, 2006, **62**, 2583–2589.
23 Z. T. Xing, H. C. Wang, Y. X. Cheng, T. D. James and C. J. Zhu, *Chem. – Asian J.*, 2011, **6**, 3054–3058.
24 X. Sun, W. Zhai, J. S. Fossey and T. D. James, *Chem. Commun.*, 2016, **52**, 3456–3469.
25 M. Faraco, D. Fico, A. Pennetta and G. E. D. Benedetto, *Talanta*, 2016, **159**, 40–46.
26 J. Yoon and A. W. Czarnik, *J. Am. Chem. Soc.*, 1992, **114**, 5874–5875.
27 H. Suenaga, M. Mikami, K. R. A. S. Sandanayake and S. Shinkai, *Tetrahedron Lett.*, 1995, **36**, 4825–4828.
28 H. Suenaga, H. Yamamoto and S. Shinkai, *Pure Appl. Chem.*, 1996, **68**, 2179–2186.
29 N. DiCesare and J. R. Lakowicz, *J. Phys. Chem. A*, 2001, **105**, 6834–6840.
30 N. DiCesare and J. R. Lakowicz, *Tetrahedron Lett.*, 2001, **42**, 9105–9108.
31 T. D. James, K. Sandanayake and S. Shinkai, *J. Chem. Soc., Chem. Commun.*, 1994, 477–478.
32 T. D. James, K. R. A. S. Sandanayake, R. Iguchi and S. Shinkai, *J. Am. Chem. Soc.*, 1995, **117**, 8982–8987.
33 S. Seraj and S. Rouhani, *J. Fluoresc.*, 2017, **27**, 1877–1883.
34 S. Rouhani and S. Haghgoo, *Sens. Actuators, B*, 2015, **209**, 957–965.
35 S. Rouhani, K. Gharanjig and M. Hosseinnezhad, *Green Chem. Lett. Rev.*, 2014, **7**, 174–178.
36 X. Sun, B. Zhu, D. K. J. Ji, Q. Chen, X. P. He, G. R. Chen and T. D. James, *ACS Appl. Mater. Interfaces*, 2014, **6**, 10078–10082.

37 J. Wang, S. Jin, S. Akay and B. Wang, *Eur. J. Org. Chem.*, 2007, 2091–2099.

38 S. Jin, J. Wang, M. Li and B. Wang, *Chem. – Eur. J.*, 2008, **14**, 2795–2804.

39 N. Dicesare, D. P. Adhikari, J. Heynekamp, M. Heagy and J. R. Lakowicz, *J. Fluoresc.*, 2002, **12**, 147–154.

40 A. M. Brouwer, *Pure Appl. Chem.*, 2011, **83**, 2213–2228.

41 R. Herráez-Hernández, P. Campíns-Falkó and J. Verdú-Andrés, *J. Biochem. Biophys. Methods*, 2002, **54**, 147–167.

42 N. I. Georgiev, I. S. Yaneva, A. R. Surleva, A. M. Asiri and V. B. Bojinov, *Sens. Actuators, B*, 2013, **184**, 54–63.

43 V. B. Bojinov, I. P. Panova and J.-M. Chovelon, *Sens. Actuators, B*, 2008, **135**, 172–180.

44 P. H. Grayshan, A. M. Kadhim and A. T. Peters, *J. Heterocycl. Chem.*, 1974, **11**, 33–37.

45 L. Xiea, J. Cui, X. Qian, Y. Xu, J. Liu and R. Xu, *Bioorg. Med. Chem.*, 2011, **19**, 961–967.

46 Q. Meng, X. Zhang, C. He, P. Zhou, W. Su and C. Duan, *Talanta*, 2011, **84**, 53–59.

47 Y. Nagao, T. Yoshida, K. Arimitsu and K. Kozawa, *Heterocycles*, 2010, **80**, 1197–1213.

48 X. Qian, Y. Xiao, Y. Xu, X. Guo, J. Qian and W. Zhu, *Chem. Commun.*, 2010, **46**, 6418–6436.

49 P. Kucheryary, R. Khatmullin, E. M. Irzakulova, D. Zhou and K. D. Glusac, *J. Phys. Chem. A*, 2011, **115**, 11606–11614.

50 Y. Fu, X. Pang, Z. Wang and H. Qu, *Molecules*, 2018, **23**, 376–390.

51 J. Zhao and T. D. James, *J. Mater. Chem.*, 2005, **15**, 2896–2901.

52 E. Watanabe, C. Miyamoto, A. Tanaka, K. Lizuka, S. Iwatsuki, M. Inamo, H. D. Takagi and K. Ishihara, *Dalton Trans.*, 2013, **42**, 8446–8453.

53 Y. Furikado, T. Nagahato, T. Okamoto, T. Sugaya, S. Iwatsuki, M. Inamo, H. D. Takagi, A. Odani and K. Ishihara, *Chem. – Eur. J.*, 2014, **20**, 1–10.

54 G. F. Whyte, R. Vilar and R. Woscholski, *J. Chem. Biol.*, 2013, **6**, 161–174.

55 U. H. Sk, A. S. P. Gowda, M. A. Crampsie, J. K. Yun, T. E. Spratt, S. Amin and A. K. Sharma, *Eur. J. Med. Chem.*, 2011, **46**, 3331–3338.

56 A. A. F. Zielinski, C. M. Braga, I. M. Demiate, F. L. Beltrame, A. L. Nogueira and G. Wo, *Food Sci. Technol.*, 2014, **34**, 38–43.

57 P. D. Duarte-Delgado, C. Narváez-Cuenca, L. Restrepo Sánchez, A. Kushalappa and T. Mosquera-Vásqueza, *J. Chromatogr. B: Anal. Technol. Biomed. Life Sci.*, 2015, **975**, 18–23.

58 R. Hadjikinova, N. Petkova, D. Hadjikinov, P. Denev and D. Hrusavov, *J. Pharm. Sci. Res.*, 2017, **9**, 1263–1269.

59 W. Xu, L. Liang and M. Zhu, *Int. J. Food Prop.*, 2015, **18**, 547–557.